Journal of Marine Systems 185 (2018) 1–12

Contents lists available at ScienceDirect

Journal of Marine Systems

journal homepage: www.elsevier.com/locate/jmarsys

Impact of offshore eddies on shelf circulation and river plumes of the Sofala Bank, Mozambique Channel

Bernardino S. Malauene[a,b,*], Coleen L. Moloney[b], Christophe Lett[c], Michael J. Roberts[d,e], Fransic Marsac[f,g], Pierrick Penven[h]

[a] Instituto Nacional de Investigação Pesqueira, Av. Mao Tse Tung 309, Maputo, Mozambique
[b] Department of Biological Sciences and Marine Research Institute, University of Cape Town, Private Bag X3, Rondebosch 7701, South Africa
[c] Sorbonne Universités, UPMC Université Paris 06, IRD, Unité de Modélisation Mathématique et Informatique des Systèmes Complexes (UMMISCO), F-93143 Bondy, France
[d] Ocean Science and Marine Food Security, Nelson Mandela University, Port Elizabeth, South Africa
[e] National Oceanography Centre, European Way, Southampton, UK
[f] ICEMASA, Department of Oceanography, University of Cape Town, South Africa
[g] IRD, UMR 248 Marbec, Avenue Jean Monnet, 34203 Sete Cedex, France
[h] Universités Brest, CNRS, IRD, Ifremer, Laboratoire d'Océanographie Physique et Spatiale, IUEM, Brest, France

ARTICLE INFO

Keywords:
Mesoscale eddies
Shelf processes
River plume
ROMS
SOMs

ABSTRACT

A high-resolution, two-way nested Regional Ocean Modeling System, forced with monthly climatologies, has been set up for the Sofala Bank and adjacent deeper ocean of the Mozambique Channel to investigate the role of offshore mesoscale eddies on the shelf circulation, hydrographic structures and river plumes. The model is shown in comparison with available observations and published studies. Most known oceanographic features are reproduced by our model. We applied Self-Organizing Maps and showed that offshore passing eddies, depending on their strength and proximity to the shelf, modulate the shelf circulation and river plume direction and spread. The presence of a strong cyclonic eddy close to the shelf induces northward surface shelf currents. In contrast, the presence of a strong anticyclonic eddy close to the shelf induces a strong southward current over most of the shelf, except off Beira. Our analyses confirm that the plume of the Zambezi River is bi-directional. The southward-directed plume patterns, opposite to the dominant northwards, occur in response to nearby offshore anticyclonic eddies (26% of occurrence). This behavior could have an influence on water dispersal, shelf ecosystems and important fisheries. Therefore, offshore mesoscale eddies should be taken into account when studying the ocean dynamics of the Sofala Bank.

1. Introduction

The Mozambique Channel, a semi-enclosed region between Madagascar and Mozambique off the African mainland (Fig. 1), is unique on a global scale because of the absence of a permanent continuous western boundary current like the Kuroshio, East Australia, Gulf Stream, Brazil or Agulhas Currents. Although currents off Pemba in northern Mozambique can show characteristics of a western boundary current (Ullgren et al., 2016) the circulation in the Mozambique Channel is dominated by trains of intermittent, passing mesoscale eddies (Biastoch and Krauss, 1999; de Ruijter et al., 2002; Lutjeharms, 2006; Sætre and da Silva, 1984; Schouten et al., 2003). Most of these eddies are a result of instabilities of the flow at the northernmost tip of Madagascar and around the narrows of the Channel at ~16°S (Backeberg and Reason, 2010; Halo et al., 2014). Although some of these eddies are cyclones, large anticyclones are the most noticeable features. Both modelling and observational studies showed that, on average, four to six large anticyclonic eddies per year occur in the Channel (de Ruijter et al., 2002; Halo et al., 2014; Schouten et al., 2003;), with diameters of ~300–400 km (Halo et al., 2014). These eddies propagate southwards at ~3–6 km day^{-1} with currents reaching up to 200 cm s^{-1} at their edges (Schouten et al., 2003). During their southward displacement, large anticyclonic eddies commonly travel along the shelf edge of Mozambique, following the topography (Halo et al., 2014; Quartly et al., 2013; Schouten et al., 2003). The shelf edge of Mozambique is therefore referred to as an "eddy corridor". The Mozambique Channel eddies, particularly dipole pairs, can generate offshore temporary boundary currents (Roberts et al., 2014; Ternon

* Corresponding author at: Instituto Nacional de Investigacao Pesqueira, Av. Mao Tse Tung 309, Maputo, Mozambique.
E-mail address: dinomalawene@yahoo.com.br (B.S. Malauene).

https://doi.org/10.1016/j.jmarsys.2018.05.001
Received 26 December 2017; Received in revised form 23 April 2018; Accepted 2 May 2018
Available online 03 May 2018
0924-7963/

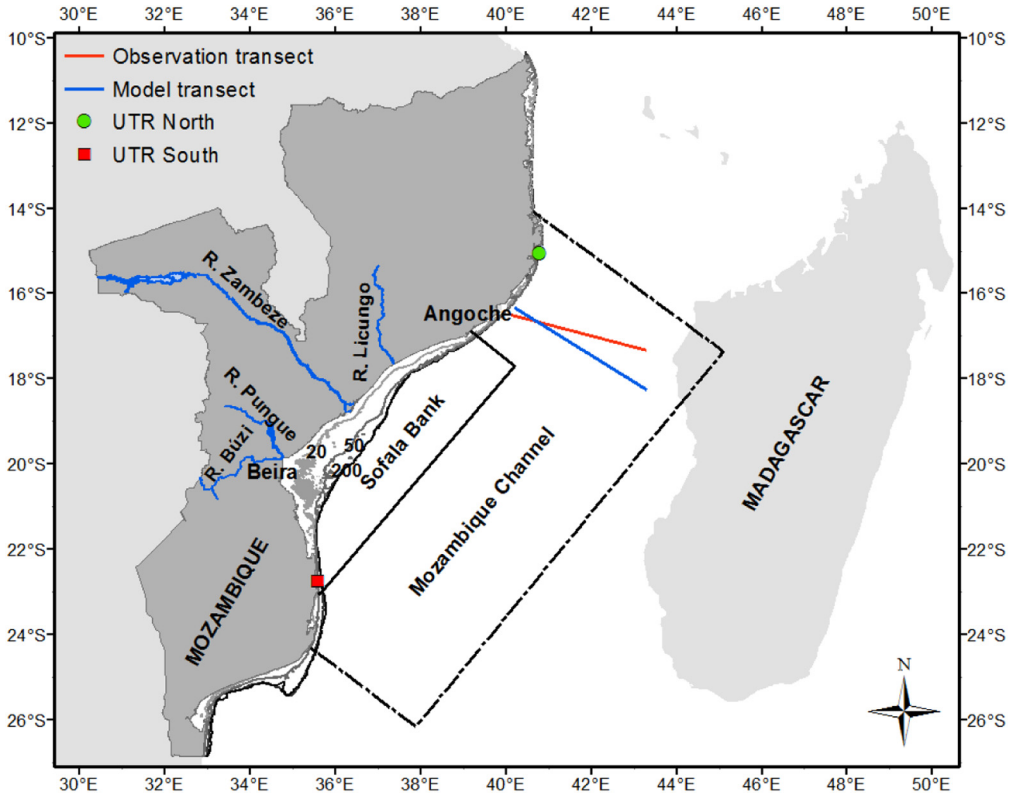

Fig. 1. Map of the Mozambique Channel with the Sofala Bank study area showing the locations of underwater temperature recorders (UTR), and the observational and model transects. Sofala Bank model domains are outlined by the black dashed-line for the large, coarse-resolution "parent" domain and the solid-line for the small, fine-resolution "child" domain.

et al., 2014). These currents have been shown to extract coastal waters offshore into the Channel (Malauene et al., 2014; Roberts et al., 2014; Tew-Kai and Marsac, 2009). The nature and magnitude of the influence of eddies on the shelf circulation and dynamics of the Sofala Bank are still unknown.

The Sofala Bank is a prominent feature in the west of the Mozambique Channel, located between 16°S near Angoche and 21°S to the south of Beira (Fig. 1). The Sofala Bank is a wide, shallow-water tropical habitat, with an average depth < 50 m (Fig. 1). The bank is characterised by strong semi-diurnal tides with highest amplitudes of up to 7 m off Beira Bay (Chevane et al., 2016). It is known to be a global "hotspot" for internal tides and wave generation (da Silva et al., 2009). Freshwater river runoff and associated river plumes are believed to influence the dynamics of marine organisms, including shallow-water shrimps, which are fished in the area. The four main rivers draining into the waters of the Sofala Bank are the Licungo, Zambezi, Pungué and Buzi Rivers (Fig. 1). The largest of these is the Zambezi River, which drains the fourth largest watershed in Africa, discharging ~3000 $m^3 s^{-1}$ (Gammelsrod, 1992). Freshwater discharge is seasonal, in relation to the rainy season, with high discharge rates between January and March and low discharge rates in October (Sætre and da Silva, 1982). Freshwater runoff from the Zambezi River generates a buoyant plume in the vicinity of the river mouth. A modelling study (Nehama, 2012) showed that the Zambezi River plume could flow both northwards and southwards, depending primarily on ambient circulation and, secondly, on the wind field. Nehama's (2012) model, however, did not include the offshore eddies of the Mozambique Channel and, therefore, their influence. Eddies presumably influence the spreading river plume and, ultimately, the distribution of sediments and organic matter, but also affect larval transport and recruitment, impacting the population dynamics of marine organisms such as shrimps. The Sofala Bank is a key natural habitat for penaeid shrimps in the Western Indian Ocean (Ivanov and Hassan, 1976), supporting an important multi-species and multi-sector shallow-water shrimp fishery. The fishery provides livelihoods for local communities and foreign income for several countries. Sofala Bank shrimps are among the main components of Mozambican export fisheries (de Sousa et al., 2013).

The aim of this study is to investigate the role of offshore Mozambique Channel eddy activity and river runoff on the ocean dynamics of the Sofala Bank, in particular shelf circulation, and the structure, direction and spread of river plumes. Because there are limited observational data, we set up a high-resolution, two-way nested model of the shelf of the Sofala Bank and adjacent open ocean using the Regional Ocean Modeling System (ROMS, Shchepetkin and McWilliams, 2005) version AGRIF (Debreu et al., 2012). Ocean models have been widely used in different regions of the world, including the Mozambique Channel (e.g. Chevane et al., 2016; Halo et al., 2014; Jose et al., 2014; Nehama and Reason, 2015; Penven et al., 2006a; Quartly et al., 2013). Most of these studies, however, focused on open waters, with little attention to the coastal and shelf regions and no modelling studies included the influences of both eddy activity and river runoff. Our model is an extension of Chevane et al.'s (2016) model, with the addition of river runoffs and a high resolution zoom on the Bank. The model results are compared with available observations and published studies.

2. Model, data and methods

2.1. ROMS for simulating ocean dynamics

We used the "Regional Ocean Modeling System" (ROMS, Shchepetkin and McWilliams, 2005) version AGRIF (Debreu et al., 2012), specifically designed for regional applications. ROMS is a three-dimensional free-surface ocean model, which solves the incompressible, hydrostatic and Boussinesq Navier-Stokes equations using a topography-following vertical coordinate system (Shchepetkin and McWilliams, 2005). This vertical coordinate system allows explicit resolution of interactions between bottom topography and ocean dynamics (Marchesiello et al., 2003), which are important for the shallow Sofala Bank. Vertical mixing is computed through a non-local K-profile

turbulence parameterization scheme (KPP; Large et al., 1994). Bottom friction is parameterised using a quadratic bottom drag term. A complete description of ROMS and its algorithms is presented by Shchepetkin and McWilliams (2005).

The two-way nesting capability of ROMS_AGRIF allows several (in this case two) model grids of different resolutions to be embedded into each other (Debreu et al., 2012; Penven et al., 2006b). In the case of two-way nesting, the fine resolution "child" model uses information from the larger scale, coarser resolution "parent" model for its lateral boundaries, and the solution of the "child" model is transferred back to update the solution of the "parent" model (Debreu et al., 2012).

2.2. Bank of Sofala Model configuration

Our ROMS-AGRIF Bank of Sofala Model (hereafter called ROMS-BSM) takes into account coastal processes such as river runoff as well as remote processes such as tides and offshore mesoscale eddy activity. Therefore, we needed a model domain large enough to encompass the entire broad continental shelf of the Sofala Bank as well as the adjacent deeper ocean (the "parent" model). At the same time, we needed a domain zoom at higher resolution, focused on the coastal shallow region of the Bank, to resolve adequately the small-scale coastal processes (the "child" model). The ROMS-BSM domain includes all four main rivers of the Sofala Bank region (Fig. 1). The "parent" model uses a structured regular grid in the horizontal plane with a resolution set to 1/16° (~6.36 km) and the "child" model resolution is 1/48° (~2.12 km). The "parent" time step is 300 s whereas the "child" time step is 100 s.

The model bathymetry is interpolated for both the "parent" and "child" grids from the General Bathymetric Chart of the Oceans (GEBCO) One Minute Grid data set (Jakobsson et al., 2008, available at http://www.gebco.net/data_and_products/gridded_bathymetry_data/, last visited April 2017). The bottom depth (h) is smoothed for numerical accuracy in order to keep an r-factor ($r = \nabla h/h$, Haidvogel and Beckmann, 1999) below 0.25. The minimum model depth at the coast is set to 30 m for the "parent" grid and 15 m for the "child" grid. This is because the tide model simulation was unstable when a minimum depth of < 10 m was used because tidal amplitudes can reach 7 m near Beira (Chevane et al., 2016). Both "parent" and "child" models have 50 vertical sigma-layers (N) with an enhanced resolution towards the surface. The vertical σ-coordinate stretching parameter at the surface (θ_s) is 5.5 and at the bottom (θ_b) is 0, and the vertical transition depth layer between the horizontal surface levels and the bottom terrain-following levels (*Hc*) is 10 m (Haidvogel and Beckmann, 1999). The bottom friction coefficient is determined by a logarithmic law with a bottom roughness of 0.01 m. The lateral explicit viscosity is zero in the interior of the domain and increases smoothly to a maximum value of 500 $m^2 s^{-1}$ in sponge layers at the lateral boundaries.

The surface forcing is defined from monthly climatologies using ROMSTOOLS (Penven et al., 2008). Wind stresses are derived from the QuikSCAT satellite gridded product at 0.25° resolution (Risien and Chelton, 2008). The climatological winds show the seasonal monsoon variation in the North and south-eastern trade winds in the South that are important for coastal processes. Heat and freshwater fluxes are derived from the Comprehensive Ocean-Atmosphere Data Set (COADS) with a 0.5° grid resolution (Da Silva et al., 1994). Sea surface temperature from Pathfinder satellite observations at ~9 km horizontal resolution (Casey and Cornillon, 1999) are used for the parametrization of the sea surface temperature feedback on the heat flux (Barnier et al., 1995).

For the lateral open boundary conditions of the "parent" model we employed the "ROMS-to-ROMS", offline nesting technique (Mason et al., 2010), using a ROMS_AGRIF solution encompassing the Mozambique Channel at 1/5° resolution (South-West Indian ocean Model: SWIM, Halo et al., 2014). The SWIM solution has been evaluated against in-situ and satellite observations as well as a HYCOM model solution and successfully reproduced the volume transport and mesoscale eddy activity in the Mozambique Channel (Halo et al., 2014). In addition, since tides are important on the Sofala Bank (Chevane et al., 2016), barotropic tides were introduced at the lateral open boundaries of the "parent" model using the ten primary tidal constituents (M2, S2, N2, K2, K1, O1, P1, Q1, Mf and Mm) derived from the Global Inverse Tide Model data set with a horizontal resolution of 1/4° (TPXO7, Egbert and Erofeeva, 2002). The tidal signal is forced into the model using a radiation condition by Flather (1976). To avoid instabilities, a ramp-up time of 2 days for the tides was applied at the initialization of the model simulation.

River discharges were incorporated into both the "parent" and "child" models as sources of momentum, heat and freshwater for the four principal river mouths: Pungué, Buzi, Zambezi and Ligungo Rivers (Fig. 1). Because the mouths of the Pungué and Buzi Rivers are located close to each other, their flows were added in the model as a single river entering Beira Bay (hereafter called "Beira-Bay River"). River flow rates (Q, $m^3 s^{-1}$) were made available by the Mozambican National Directorate of Water (DNA) as monthly-averaged climatologies from 1963 to 1977 and fitted into the model as a constant monthly flow. River temperatures and salinities were derived from averaged temperature (28 °C) and salinity (20 psu) collected by the Mozambican National Institute of Fisheries Research (IIP) annual cruise surveys between 2003 and 2010.

2.3. Data

Independent in situ and satellite data, not used in the model configuration, were used to assess the accuracy of the model solutions and to identify oceanic features. Observational data are scarce in the Mozambique Channel, particularly on the Sofala Bank. Underwater temperature recorders (UTR-model Seamon mini temperature recorder, accuracy ± 0.01 °C) deployed at a depth of 18 m in the South (~23 °S) and in the North (~15 °S) of the Sofala Bank (Fig. 1) were available for the study. The UTRs recorded hourly measurements of temperature from 2001 to 2007. Hourly data were averaged into monthly climatology time series, and then analysed.

Altimetry data obtained from multi-satellite observations were used for the circulation and mesoscale eddy fields, specifically: (i) Sea Surface Height (SSH) derived from absolute dynamic topography (ADT) product produced by Ssalto/Duacs (Ducet et al., 2000) and (ii) Geostrophic current with mean dynamic topography (MDT) produced by CLS (Rio et al., 2011). Both products were weekly and were gridded at 1/4° resolution for the period 1993–2008, and were distributed by AVISO, with support from CNES (http://www.aviso.oceanobs.com/, last visited September 2017).

2.4. Plume index

A freshwater plume index (h_f) of thickness was used to determine the extent of the river plumes on the Sofala Bank. The index is defined as the vertical integration of a salinity anomaly by the expression $h_f = \int_{-H}^{\eta}((S_0 - S)/S_0)d_z$ (Hetland, 2004; Horner-Devine, 2009), where −H is the bottom depth, η the free surface and So is the reference salinity on the Sofala Bank (S_0 = 34.5 psu).

2.5. Self-organizing maps

We used self-organizing maps (SOMs) to illustrate several typical cases of interactions between eddies in the Mozambique Channel, the currents on the Sofala Bank and river plumes. SOMs also have been used in studies in other regions of the world (South China Sea, Liu et al., 2008; East China Sea, Jin et al., 2010; Adriatic Sea, Falcieri et al., 2014; Gulf Stream, Zeng et al., 2015). SOMs constitute an artificial neural network classification method and a non-linear cluster analysis (Kohonen, 2001). SOMs project complex, multi-dimensional (large)

input data into low-dimensional (in this case two-dimensional) output maps, so-called patterns or units (Kohonen, 2001). The unit showing the smallest Euclidean distance is the "winner" at best representing and preserving the input data, i.e., the best matching unit (BMU).

We applied unsupervised SOMs, in which no preselected patterns are chosen, to the modelled SSH and salinity fields, in order to identify and extract patterns of mesoscale eddy activity and river plumes on the Sofala Bank. Prior to performing the SOMs training, the model SSH data were reprocessed to SSH anomalies by subtracting the mean, whereas salinity was converted into a freshwater plume index as described above. The training parameters were chosen according to Liu et al. (2006) and included a rectangular neural lattice of "flat sheet" shape, linear initialization, "ep" neighborhood function with radius of 1, and the "batch" algorithm. The relative frequency of occurrence of each pattern was computed based on the BMU time series and given as a percentage in the SOMs. The SOMs analyses were performed using R package Kohonen (Wehrens and Buydens, 2007).

3. Results

The model was run for 10 years with outputs averaged every three days. The model spin-up was three years, defined by the volume-averaged salinity, which was the last variable to reach an equilibrium stability (not shown). Thus, the model solution available for analysis is seven years long (year 4–year 10).

3.1. Comparison of model with observations

Assessment of the realism of our model solutions was carried out, where possible, by comparisons with observational data and knowledge gained from the available literature. Here we focus on accurate reproduction of mean state of eddy dynamics, currents and salinity, and seasonal temperature.

3.1.1. Mean eddy variability

Mean root mean square (RMS) of SSH computed from the model exhibited a maximum in the central Mozambique Channel (Fig. 2A), in agreement with those from AVISO altimetry observations (Fig. 2B). However, the maximum value of modelled RMS was ~35 cm, whereas the AVISO maximum was ~20 cm, suggesting the model overestimated eddy variability. There was a decrease from the offshore maximum to a minimum on the shelf, with a strong gradient (closely-spaced contours) that ranged 5 cm for both model (20–15 cm) and AVISO (15–10 cm) (Fig. 2). The gradient followed the slope topography.

3.1.2. Mean surface currents

The presence of a mean Mozambique Current is still the subject of debate (Lutjeharms et al., 2012), but ROMS-BSM mean surface currents agreed with observations distributed in CNES-CLS09 products (Fig. 3). In particular, there was a strong agreement regarding an alongshore, poleward mean current, following the 200 and 2000 m isobaths over the slope. Also, the strongest mean surface current occurred in the North (~16°S) and in the South (~22°S) in both model and observations. However, the modelled mean currents were faster (up to 100 cm s^{-1}; Fig. 3A) than CNES-CLS09 observations (up to 70 cm s^{-1}; Fig. 3B). There were weak current velocities on both the inshore and offshore sides of the strong mean poleward current for the model as well as for the observations (Fig. 3). Offshore, the mean surface current was found to flow in an equatorward direction.

3.1.3. Mean vertical current sections

Because of the scarcity of observational data on currents in the vertical plane on the Sofala Bank, model realism was investigated by taking into consideration knowledge gained from the Long-term Ocean Climate Observation (LOCO) program (Ullgren et al., 2012) and the "parent" model. The vertical distribution of long-term mean alongshore velocity from our 7-year ROMS-BSM simulations (Fig. 4A) was consistent with the vertical current patterns known from the 6-year LOCO observations (Fig. 4B). In particular, the following three main currents were reproduced by the model (Fig. 4): (i) a strong, slope, mean poleward surface current on the western side (as already noticed on the horizontal plane, Fig. 3), (ii) a weaker mean equatorward surface current on the eastern side (as already noticed on the horizontal plane, Fig. 3) and (iii) a mean equatorward undercurrent known as the Mozambique Undercurrent, from 750 to 1000 m depth, below the poleward surface current.

A vertical section of the modelled, long-term mean salinity showed isohalines uplifting on the continental slope in the upper 500 m on the west side of the Channel (Fig. 4C). There was a modelled deep salinity minimum (< 34.7) between 1200 and 1600 m depth on the western side of the Channel (Fig. 4C), which is in agreement with the LOCO salinity observations (Fig. 4D).

3.1.4. Seasonal temperature

Modelled monthly-averaged bottom temperature at 18 m depth was in agreement with UTR observations at the South and North of the Bank (Fig. 5; Table 1). The model reproduced the clear observed seasonal temperature variations with a range of ~4.5 °C from summer to winter at both locations (Fig. 5A and B). There was a significant correlation between the two time series in the South (r = 0.96) and in the North (r = 0.84). However, the modelled mean temperatures were slightly

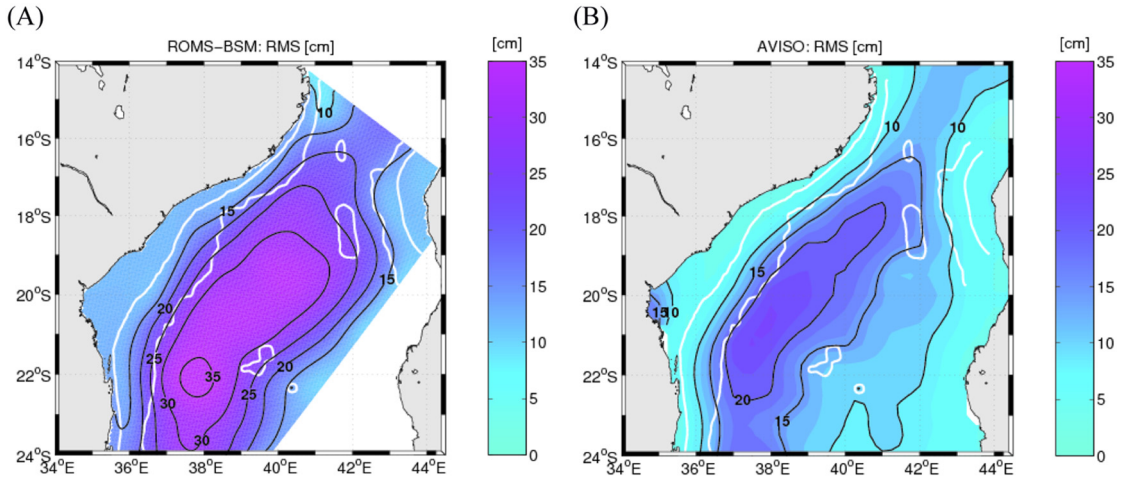

Fig. 2. Comparison of mean RMS computed from SSH (cm) between (A) ROMS-BSM model and (B) AVISO observations. Grey contours are 200 and 2000 m isobaths.

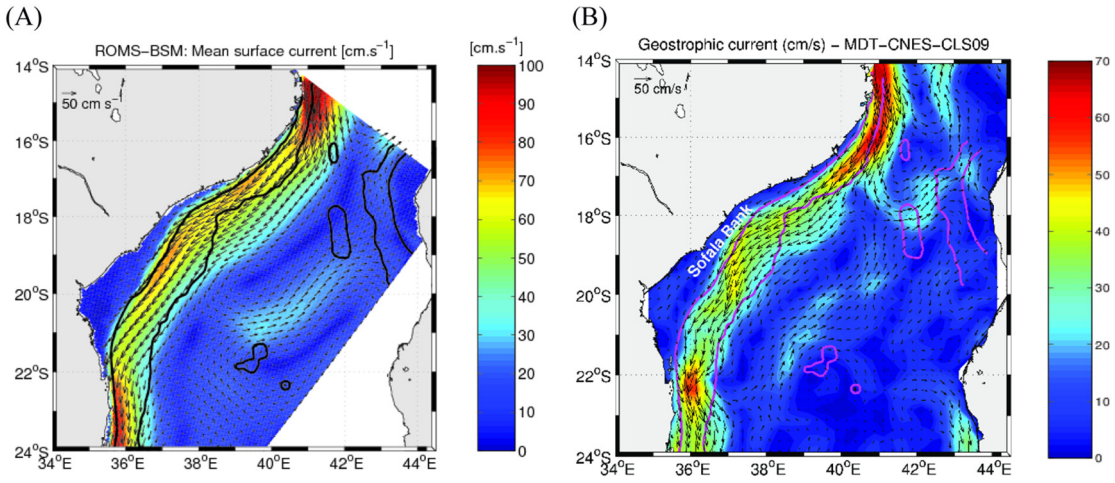

Fig. 3. Comparison of long-term mean surface currents (cm s^{-1}) between (A) ROMS-BSM model and (B) MDT-CNES-CLS09 observations. Grey contours are 200 and 2000 m isobaths. Note that the model and observations are plotted with a different vectors scale and colorbar for better visualization.

warmer compared to the observations, by ~0.35 °C in the South and ~1 °C in the North (Table 1). In the North, the difference was larger during the summer (2–3 °C in November–February) than in winter (< 0.5 °C) (Fig. 5B).

3.2. Offshore eddy variability patterns using SOMs

A set of preliminary experiments with different SOMs sizes was used to select a 3 × 4 SOMs map size with 12 patterns, as this map size gave the most useful, detailed information. SOMs based on seven years of modelled sea surface height anomaly (SSHA) fields showed mesoscale eddies with variable dynamics, including anticyclonic, cyclonic, dipole

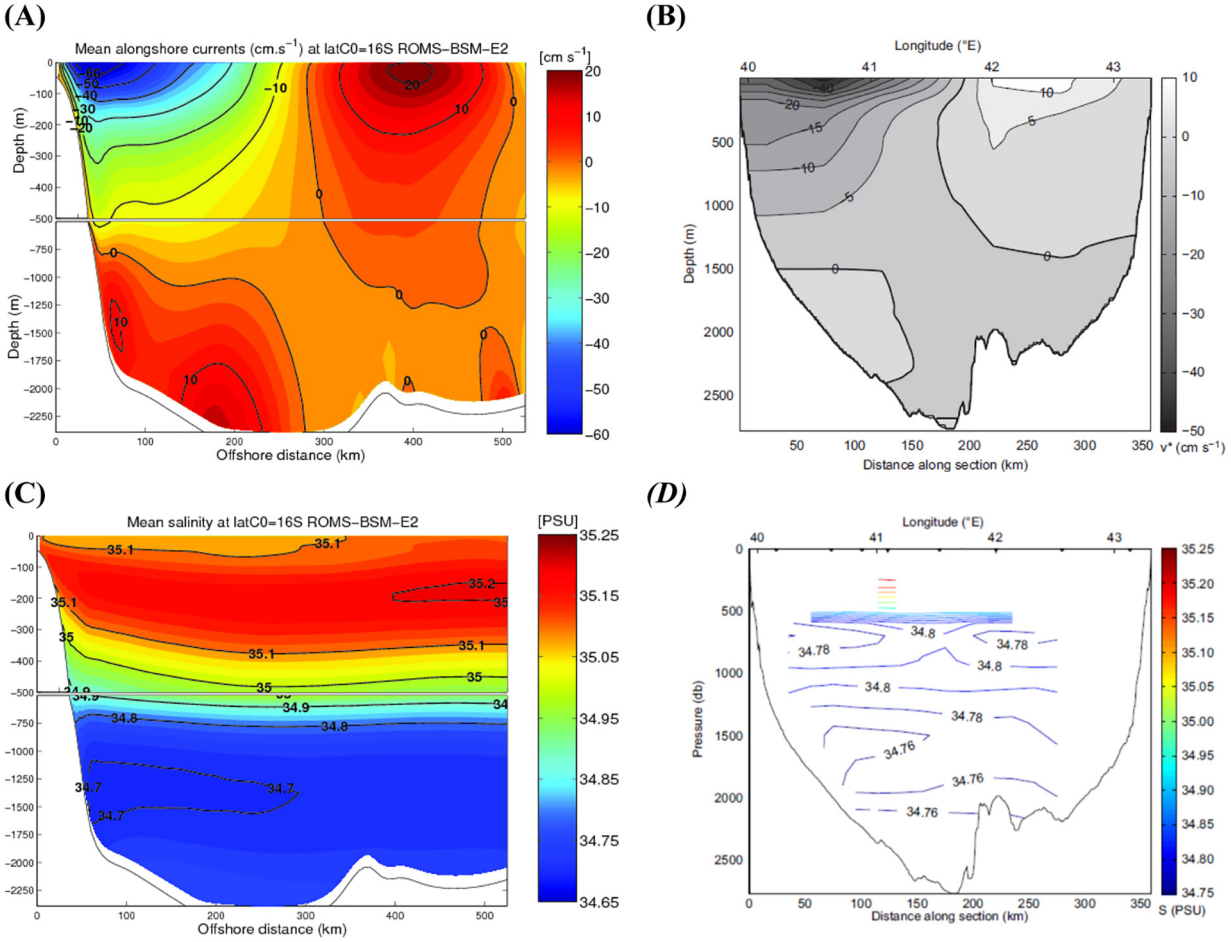

Fig. 4. Comparison of long-term mean vertical cross-shelf transect for: (A and B) alongshore velocity (cm s^{-1}) and (C and D) salinity (psu), between (A and C) ROMS-BSM model and (B and D) Long-term Ocean Climate Observation (LOCO) for the period 2003–2009 (Ullgren et al., 2012). Transect locations as in Fig. 1.

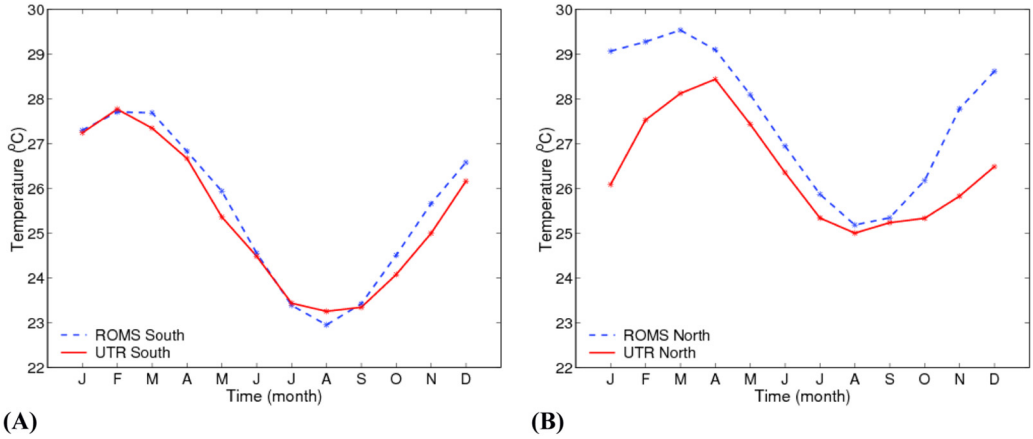

Fig. 5. Comparison between ROMS-BSM model (dashed-line) and UTR observations (solid-line) monthly mean temperature (°C) at 18 m depth in (A) southern and (B) northern UTR sites as in Fig. 1.

Table 1
Correlation coefficient (r), bias and root mean square error (RMSE) of comparisons between ROMS-BSM model and UTR observed monthly mean temperature (°C) at 18 m depth in southern and northern UTR sites as in Fig. 1.

ROMS vs UTR	r	Bias (°C)	RMSE
South	0.99	0.20	0.34
North	0.84	1.15	1.43

and tripole eddies (Fig. 6A). Anticyclones dominated the eddy patterns, with higher SSHA amplitudes (0.6 m) than for the cyclonic eddies (−0.4 m). The SOMs indicated two patterns of eddy generation, namely 2 (11% of occurrence) and 6 (8% of occurrence), that had weak SSHA and preceded the well-developed eddy patterns — respectively 1 (6% of occurrence) and 5 (12% of occurrence) (Fig. 6A). In contrast, other SOMs represented an eddy decay pattern, particularly 11 (11% of occurrence), with weak SSHA following the well-developed eddy patterns of 5 (12% of occurrence) and 10 (10% of occurrence).

There is no seasonal variability shown in the modelled BMU time series of eddy patterns (Fig. 6B). However, the BMU analysis does show that these eddies mostly propagate progressively southward and westward. An example is given by following the pattern sequence $12 \underrightarrow{\rightarrow} 1 \rightarrow 5 \rightarrow 10 \rightarrow 11$ at the beginning of the BMU time series (Fig. 6B). In pattern 12, there is an anticyclonic eddy in the south at ~21°S and 38°E (Fig. 6A), while another anticyclonic feature enters the domain from the north. In pattern 1, the southern anticyclone has moved southward and the northern anticyclone, once developed, also moves south. The low negative SSHA between the two anticyclones indicates a cyclonic eddy which similarly moves southward. In pattern 5, the southern anticyclone exits the study domain to the south, while the northern anticyclone continues to move southward. In pattern 10, the anticyclonic eddy to the north moves westward. Finally, in pattern 11, the anticyclone from the north decays near the central Sofala Bank.

3.3. Offshore eddy influences on the shelf circulation

Composite-averages of modelled surface currents during the period of each SSHA SOM pattern in the BMU time series (Fig. 6) were produced to investigate the influence of the Channel eddies on the shelf circulation (< 200 m). Here, we focus on the composites for selected patterns of cyclonic, anticyclonic and dipole eddies located off the central Sofala Bank. Special attention is given to eddy strength and proximity to the shelf.

3.3.1. Effect of cyclonic eddies

A strong cyclonic eddy close to the shelf (pattern 1 in Fig. 6) corresponded to an average shelf surface current directed to the North (Fig. 7A), opposite to the mean southward flow (Fig. 3). This northward current appeared over most of the shelf and reached the coast, except off Beira (~20°S) where there was a weak and, at times, southward current (Fig. 7A). A weak cyclonic eddy (pattern 2 in Fig. 6) was similarly associated with a northward current on the shelf, but in a narrow band along the shelf-break that did not reach the inner shelf (not shown).

3.3.2. Effect of anticyclonic eddies

A strong anticyclonic eddy close to the shelf (pattern 7 in Fig. 6) was associated with a southward shelf current (Fig. 7B). This current was strong over most of the shelf up to the coast, except off Beira. When the anticyclone was found further offshore (pattern 9 in Fig. 6), a narrow southward current was found on the shelf-break, with limited effects on the inner shelf (not shown).

3.3.3. Effect of an eddy dipole

For a dipole eddy pair with the cyclone to the North (pattern 4 in Fig. 6), a strong inshore surface current bifurcated into northward and southward branches between the two eddies on the shelf-break (at ~19°30′S), in accordance with the rotations of eddies (Fig. 8A). In contrast, for an eddy dipole with the anticyclone to the North (pattern 10 in Fig. 6), there was a southward current to the North and a northward current to the South, converging into a strong offshore current (Fig. 8B).

3.4. River plume variability patterns using SOMs

Similar to the SSHAs, the SOMs applied to seven years of a river plume index derived from modelled salinity appeared to provide the best information with a 3 × 4 map size (not shown). These showed that the model captured the freshwater plumes of the three river sources on the Sofala Bank, i.e. the Beira Bay rivers (Pungué and Buzi combined), Zambezi River and Licungo River (Fig. 9A). Note that the plumes of the Licungo River and off Beira Bay are not clear in Fig. 9 because of the scales used. Because these river plumes are not the focus of this study, they will not be discussed in detail and the main focus will be the Zambezi River plume.

The Zambezi River plume, being the largest freshwater input, had the strongest impact, spreading over the largest area (Fig. 9A). The dominant structure of the Zambezi plume was oriented northward and was narrow and attached to the coast, particularly when furthest (> 150 km) from the river mouth. In SOM patterns 1, 2, 3, 5, 6, 9 and 10 there was a bulge-like structure associated with the plume, which expanded offshore. Patterns 1, 2, 3 and 5 (summed 25% of occurrence)

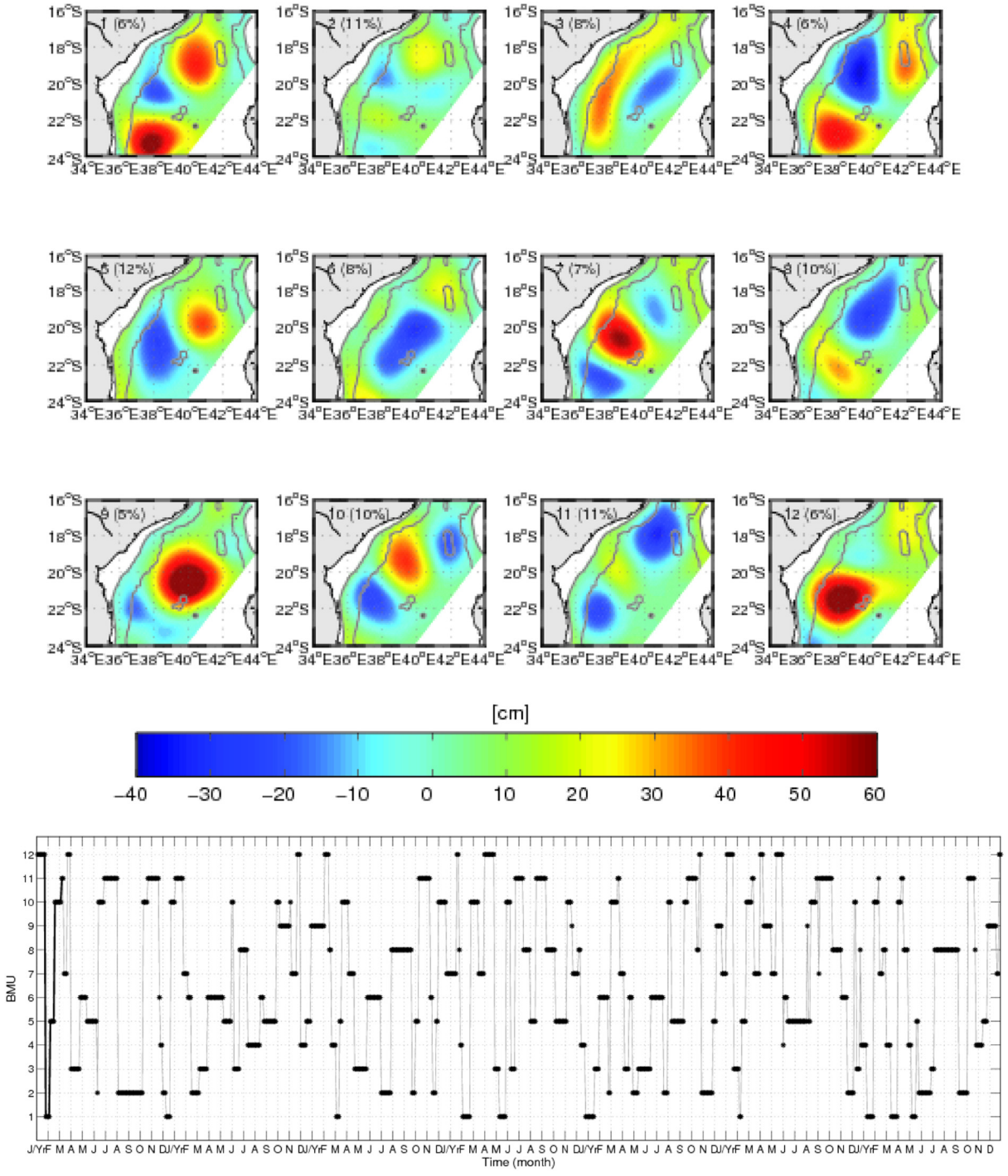

Fig. 6. (A) 3 × 4 SOMs of simulated SSH anomaly. The shelf region within the 200 m depth was masked for a better representation of the offshore eddies. Blue (negative) SSHA core indicates cyclonic eddies and red (positive) SSHA anticyclonic eddies. The numbers 1–12 (in the top left corner) indicate the SOMs patterns and the percentage (in brackets) are corresponding frequency of occurrence in seven years (4–10). (B) The best matching unit (BMU) for the temporal evolution of the 12 patterns in (A). Black line (beginning of the time series) highlights a sequential event of eddies propagating southwards.

illustrated cases of river plumes that were southward-oriented and were detached from the coast (Fig. 9A).

In accordance with reality, the BMU time series showed a clear seasonal cycle in the modelled plume variability (Fig. 9B). Large plumes (1, 2, 3, 4 and 7) occurred in January–May during the rainy season. Plume patterns 5, 6, 8, 11 and 12 occurred in June–August and December, during the transition between the rainy and dry seasons, whereas the smallest plume patterns 9 and 10 were in September–November during the dry season. Of all the SOMs, pattern 9 showed the most offshore (> 50 km from the coast) spread of the Zambezi plume, but its frequency of occurrence was the smallest (2%). The small-bulge pattern 10 accounted for the largest frequency of occurrence (~22%), covered most of the dry season and was found over a long period of > 60 consecutive days (Fig. 9B).

3.5. Influence of offshore eddies on river plume variability

In order to investigate the influence of the offshore eddies on the

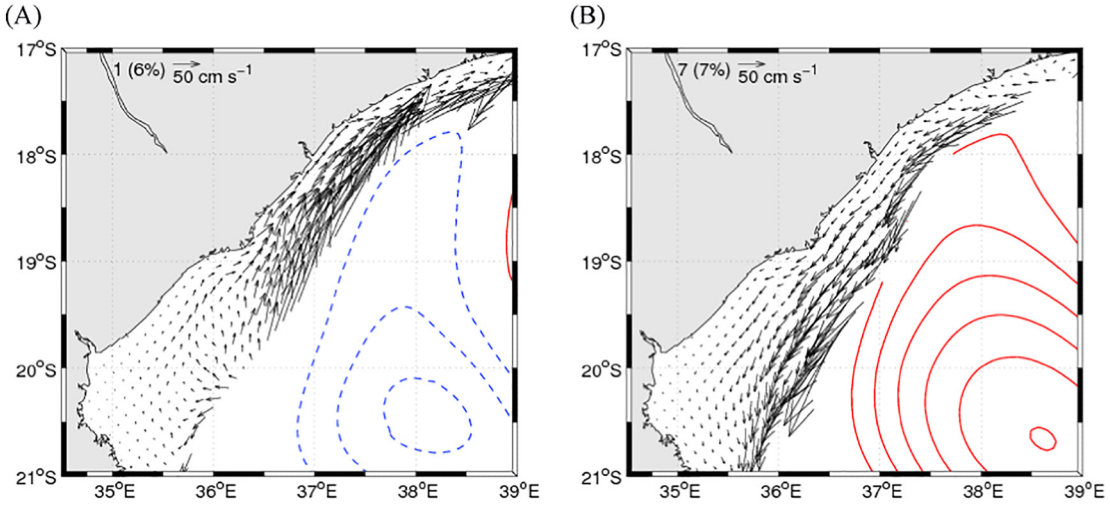

Fig. 7. Averaged surface shelf currents when (A) a strong cyclonic eddy is close to the coast and (B) a strong anticyclonic eddy is close to the coast as shown in the upper left corner pattern and frequency of occurrence in Fig. 6A. Contours in 10 cm intervals indicate (blue) cyclonic eddy and (red) anticyclonic eddy. The domain has been cropped from the SOM map and the current outside 200 m isobath masked to improve visualization of the shelf circulation. (For interpretation of the references to colour in this figure legend, the reader is referred to the web version of this article.)

Zambezi River plume, modelled SSHAs were averaged over the period of each plume SOM pattern in the BMU time series. Modelled southward-directed river plumes were mostly associated with a well-defined offshore mesoscale eddy, generally an anticyclone in both summer (patterns 1, 2 and 3) and winter (pattern 5) (Fig. 9). The plume patterns 1 and 5, which had a long southward incursion that extended past ~19°S (Fig. 9A), were related to an anticyclone that was strong (SSHA > 0.6) and close to the shelf (Fig. 9). In contrast, river plume patterns 2 and 3, which had shorter southward excursions, were related to an anticyclone being farther offshore and weaker (SSHA < 0.4) (Fig. 9). For the other river plume patterns, we did not find a clear relation between the plume pattern and the eddy activity, apart from generally weak SSHA features (Fig. 9).

4. Discussion

We implemented a high-resolution, two-way nesting, climatological ocean model for the Sofala Bank and adjacent deep ocean in the Mozambique Channel. The modelled mesoscale circulation and hydrographic structures were in general agreement with observations and literature. We found strong effects of offshore eddies on the shelf circulation and river plume structures.

4.1. Model-observation comparisons

Comparisons of RMS of SSH from ROMS-BSM (Fig. 2A) and from AVISO observations (Fig. 2B) were in reasonable agreement. This indicates that the model reproduces the highly energetic eddy variability of the Mozambique Channel (de Ruijter et al., 2002; Lutjeharms, 2006; Sætre and da Silva, 1984; Schouten et al., 2003; Tew-Kai and Marsac, 2009; Weimerskirch et al., 2004). The structure of modelled RMS SSHs over the Mozambican continental slope between the 200 m and 2000 m isobaths is a signature of the "eddy corridor" (Halo et al., 2014; Schouten et al., 2003), indicating that the model generates the eddies at a realistic location and frequency. The elevated mean eddy variability in the model compared to the AVISO altimetry (by ~40% RMS) could be explained by an overestimation of the eddies in the model and/or by the coarser resolution of the AVISO altimetry data, which are thus not able to represent the full realistic aspects of the eddy field. The variability also could be caused by the outputs from the SWIM model that were used for the open boundary conditions and propagated throughout our model. SWIM overestimates the Mozambique Channel eddy variability relative to AVISO by about 40–50% (Halo et al., 2014), because modelled eddies have larger diameter and greater amplitude than AVISO. Nonetheless, SWIM was useful for simulating Mozambique

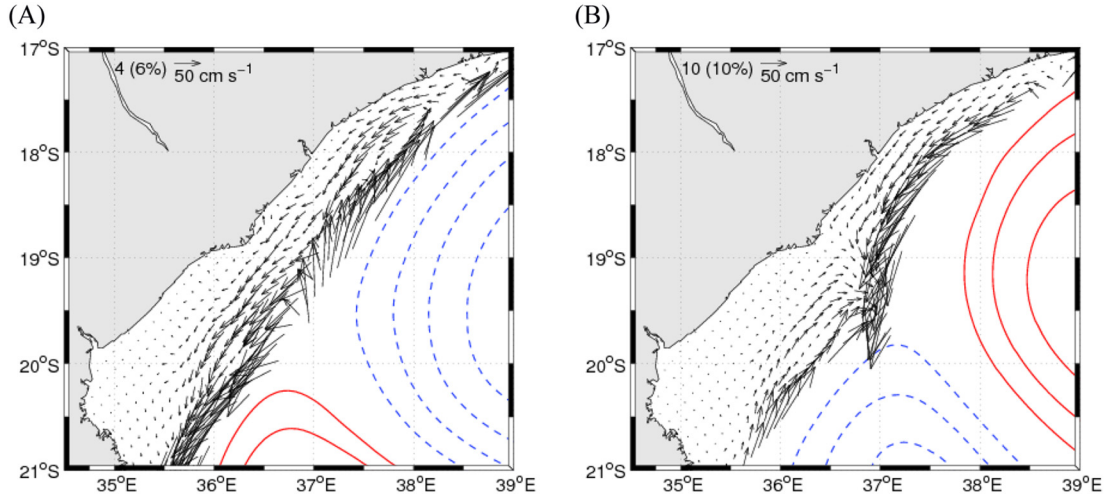

Fig. 8. Same as Fig. 7 but relative to dipole pair of eddies (A) cyclone – anticyclone (pattern 4) and (B) anticyclone – cyclone (pattern 10).

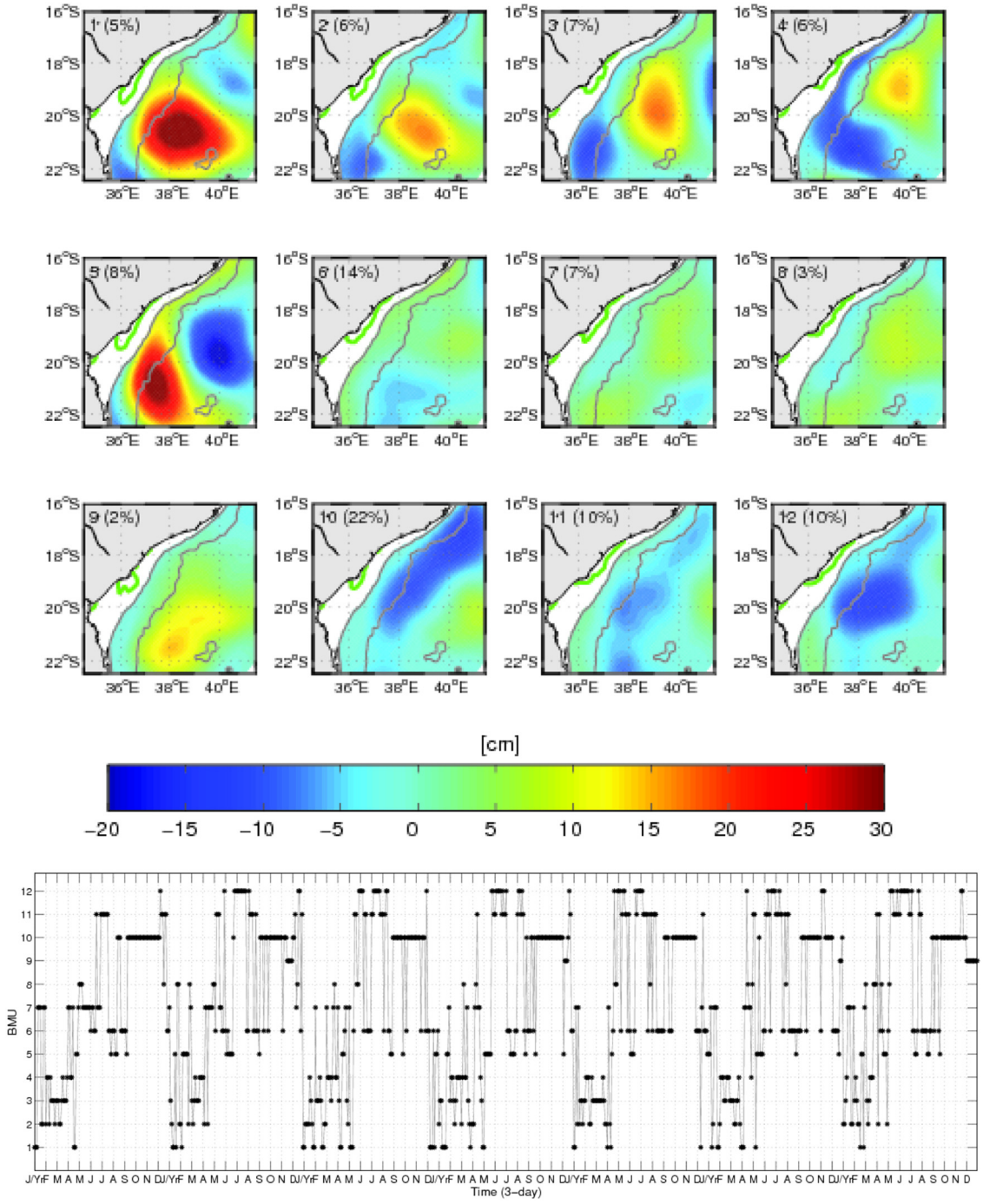

Fig. 9. Same as in Fig. 6, but for 3 × 4 SOM of simulated river plume index (outlined by green line) overlaid with corresponding modelled SSHA (color shading) averaged over the period of each plume SOM pattern in the BMU time series to indicate eddy activity. Grey contours are 2000 m isobaths and the area inside 200 m isobath is masked. (For interpretation of the references to colour in this figure legend, the reader is referred to the web version of this article.)

Channel eddies, which were missing in other models of the region (e.g. Nehama, 2012).

The model reproduced the presence of a surface poleward "mean Mozambique Current", in agreement with other recent model simulations (Lutjeharms et al., 2012). Classic understanding, prior to the 1980s, was that a permanent western boundary current existed along the continental slope of Mozambique. Nowadays, however, it is known that the circulation in the Mozambique Channel is dominated by intermittent southward-migrating mesoscale eddies (Biastoch and Krauss, 1999; de Ruijter et al., 2002; Lutjeharms, 2006; Penven et al., 2014; Ridderinkhof and de Ruijter, 2003; Sætre and da Silva, 1984; Schouten et al., 2003). The long-term average of temporal poleward flows produced in the eddy corridor could indeed suggest a "mean Mozambique Current" on the slope (Fig. 3), but such a current may also be related to southward-propagating eddies.

The elevated model surface currents can also be explained by the greater horizontal resolution (6 km) of the model compared to the global, smoothed and coarser resolution of CNES-CLS09 observations (25 km). Increasing the resolution of models will generally improve their ability to represent realistic aspects of the mean "Mozambique Current" flow (Quartly et al., 2013). The model used for our open boundaries (SWIM) also overestimates transport across the

Mozambique Channel (Halo et al., 2014). This could result in a stronger mean Mozambique Current along the slope. In the Mozambique Channel, surface current velocities derived from altimetry (AVISO) were found to underestimate velocities observed from ship-ADCP and from surface drifters by ~30% (Ternon et al., 2014), corroborating our results.

The vertical section of modelled mean alongshore currents and hydrography corroborated the surface current patterns, in particular, the mean "Mozambique Current" depicted by the strong southward current (Ullgren et al., 2012) and isoclines of temperature and salinity uplifted in the upper 500 m. However, LOCO, which is the longest in situ dataset in the region, lacks hydrographic sampling in the upper 500 m (Ullgren et al., 2012), making it difficult to evaluate the model hydrography in this layer. This highlights the relevance of ocean models in a region where observations are scarce. In the intermediate waters (1500 m) the model showed an equatorward current, with a corresponding salinity minimum (Fig. 4), in agreement with LOCO observations (Ridderinkhof and de Ruijter, 2003; Ullgren et al., 2012). A snapshot transect of current measured by L-ADCP (Lowered Acoustic Doppler Current Profiler) also showed a similar structure (de Ruijter et al., 2002), corroborating our model. A NEMO model-based study also found similar vertical current structures using a coarser (1/4°) resolution, but the undercurrent appeared distorted when a higher-resolution (1/12°) was used (Quartly et al., 2013). In contrast, the present model, using a finer resolution (1/16°), showed a clear Mozambique Undercurrent which matched the observations (de Ruijter et al., 2002; Ullgren et al., 2012), confirming that our model represents the vertical currents reasonably well.

The model reproduced the observed seasonal temperature variations on the southern and northern Sofala Bank (Fig. 5; Table 1). However, an apparent difference in the modelled temperature occurred in the North during the summer. Malauene et al. (2014) showed that partly wind-induced cool water upwelling is observed on the northern Sofala Bank near Angoche, occurring as quasi-synoptic intermittent events during the summer northeastern monsoon. This coincides with cooler summer waters observed at the Northern UTR than in the model. This discrepancy could be explained by the use of monthly climatological QuickScat wind forcing, which lacked the temporal high-resolution necessary to adequately reproduce the quasi-synoptic Angoche upwelling events. It also could be influenced by a mismatch in scale between the applied climatologies and the UTR data. Similar differences in the reproduction of observed summer cooling are reported in the Zanzibar Channel Model, also using ROMS (Zavala-Garay et al., 2015).

4.2. Offshore eddy variability and influence on shelf circulation

The 3 × 4 Self-Organizing Maps analysis of Sea Surface Height (SSH) anomaly confirmed that the model captured the eddy variability in the Mozambique Channel. There were both anticyclonic and cyclonic eddies, with the former being dominant in terms of amplitude. Identified patterns 1, 4, 7 and 10 (Fig. 6A) showed a succession of cyclonic and anticyclonic eddies, i.e. eddy dipoles and at times tripoles, over the continental slope of Mozambique. This is coherent with previous studies, based on empirical orthogonal function analyses computed on satellite altimetry, that showed the variability in the mesoscale eddy pattern in the Mozambique Channel is explained by dipoles (10% variance; Tew-Kai and Marsac, 2009) or tripoles (15% variance; Schouten et al., 2003).

The temporal evolution of the modelled eddy patterns, as represented by time series of the best matching unit (BMU), captured the southward propagation of these eddies (Fig. 6B), in agreement with previous studies (de Ruijter et al., 2002; Lutjeharms, 2006; Sætre and da Silva, 1984; Schouten et al., 2003; Tew-Kai and Marsac, 2009). Weak positive and/or negative SSH anomalies emerged before well-developed anticyclonic and/or cyclonic eddies formed, indicating the early phase of an eddy. This confirms that, although most of the eddies are generated to the north of the Mozambique Channel between the northernmost tip of Madagascar and the Comoros (Backeberg and Reason, 2010; Halo et al., 2014), some anticyclonic and cyclonic eddies are also generated locally within the Channel (Halo et al., 2014). There were weak SSH features after well-developed eddies, indicating that some eddies could also dissipate (decay) locally, near the Sofala Bank.

Our study confirmed that modelled offshore mesoscale eddy activity in the Mozambique Channel can strongly modulate the adjacent shelf circulation on the Sofala Bank (Figs. 7 and 8). The eddy rotation (type) plays a critical role in modulating the variability of the flow direction. There were cyclonic eddy-induced equatorward shelf currents, opposite to the southward net flow (Fig. 7A). In contrast, anticyclonic eddies induced strong poleward surface currents (Fig. 7B). A similar anticyclonic eddy-induced current was found in the South China Sea, influencing the western boundary Kuroshio Current (Cai et al., 2002). In our case there is no western boundary current, thus eddies influence directly the shelf and coastal currents.

The proximity of the offshore eddy, either cyclone or anticyclone, to the shelf, also played a role in circulation; eddies close to the shelf strengthened currents over most of the shelf, whereas eddies farther offshore had limited influence on the shelf, with the exception of a narrow shelf-break zone. These results imply that, for eddies far offshore, the transferred energy is dissipated before it reaches the inner-shelf. Further south of the Sofala Bank (at ~20°S), a poleward surface current was reported that decreases in intensity from the edge of an offshore anticyclonic eddy towards the coast (Roberts et al., 2014). Diminishing influence of eddies to the west was also found to be related to the eddy strength, such that strong eddies intensified the shelf circulation up to the coast, whereas weak eddies had some influence over the shelf-break but less on the inner-shelf.

Off Beira the mean circulation was weak, independently of the eddy activity, indicating that this region was not influenced by offshore eddies. Possibly, the wide and shallow shelf made it difficult for eddy-related current velocities to affect the coastal areas, and the energy dissipated by eddies was converted to generate internal waves at the slope-shelf interface. Strong tidal mixing and currents (up to 70 cm s^{-1} during the spring tides Chevane et al., 2016) could also have dominated the influence of far offshore eddies.

Dipole pairs of eddies also strongly influenced the shelf circulation, with opposite current directions according to the counter-rotation relative to the dipole. Eddy dipoles with the anticyclone (cyclone) to the North induced strong poleward (equatorward) currents on the North of the dipole axis and equatorward (poleward) currents on the South. This resulted in current convergence (divergence), with a strong offshore (inshore) current between the two eddies. Snapshots of observed coastal ship-ADCP currents showed a similar strong current towards the shore (offshore) associated with the eddy dipole (Roberts et al., 2014; Ternon et al., 2014). In these observational studies, as in the present model, the contribution of the anticyclonic eddy dominated the cyclone counterpart. This possibly occurred because anticyclonic eddies in the Channel are generally larger and stronger than cyclones (Halo et al., 2014).

4.3. River plume variability and influences of offshore eddy

Modelled plume index computed from salinity using SOMs confirmed that the Zambezi River plume is frequently bi-directional (Fig. 9), extending both north and south (Nehama, 2012; Nehama and Reason, 2015). The plume was dominantly northward-directed, closely attached to the coast in a narrow band with a far penetration to the North (> 150 km) (Fig. 9). This is caused by the Coriolis force (Garvine, 1987) which, for the southern hemisphere, deflects the freshwater outflow to the left of the river mouth and keeps it attached to the coast. We did not found a significant relationship between the northward plume and offshore eddies (Fig. 9), supporting the notion of the Coriolis

force as the main driving force for this plume direction.

In contrast, the southward-directed plume was clearly detached from the coast and directly related to offshore anticyclonic eddies (Fig. 9). In order for a bi-directional plume to occur, a current that dominates the Coriolis tendency is required to deflect the plume in the opposite direction, such as described for a wind-driven current (Hickey et al., 2005). For the Zambezi plume, it was shown that winds play a minor role in its variability (Nehama, 2012) but large anticyclonic eddies were able to induce a southward current over most of the shelf (Fig. 7B), resulting in southward-directed plumes (Fig. 9). Hence, the proposed mechanism is that offshore anticyclonic eddies eroded the dominant coastal northward plumes and reversed them to the south. In this case, the Coriolis force maintained the southward branch detached from the coast. Interestingly, in the region off Beira (~20°S), which is protected by the bay and has limited influence by offshore eddies, the Pungué and Buzi combined plume is mainly uni-directional (Fig. 9A).

We found a clear seasonal pattern in the modelled plume structure (Fig. 9). Consistently, larger average plumes occurred in summer to autumn during the high river discharge rates season and smaller ones in winter to spring at times of low discharge rates. This indicates seasonal variations of the river plume in relation to the seasonality in river discharge. Caution needs to be exercised when interpreting this modelled seasonality of the Zambezi River plume because the river flows used as input to the model were from 1973 to 1977 and may not reflect the influence on the seasonal signal of the Cahora Bassa Dam in Mozambique (built between 1969 and 1974) and other upstream dams. Based on observations of CTD salinity data during high river discharge seasons in summers from 2004 to 2007, the plumes were generally large and decreased in size during the year, together with river discharge (Nehama, 2012; Nehama and Reason, 2014), corroborating our findings. The most persistent plume pattern (22%) was obtained during the dry season, indicating consistent plume structure during the low river-discharge period. The period of high river-discharge showed highly variable plume structures, as found for the Po River plume in the Adriatic Sea (Falcieri et al., 2014).

Overall, this study confirmed that the Sofala Bank Model is comparable with observations and provided new information on shelf circulation, hydrographic structures, river plumes and their drivers. The Sofala Bank Model can therefore be applied for interdisciplinary studies, such as addressing the influences of offshore eddies and circulation to improve our understanding of dispersal patterns of coastal marine species and their population dynamics.

Acknowledgments

This work was supported by French Agence Inter-établissements de Recherche pour le Devéloppement (AIRD-DPF); International Center for Education, Marine and Atmospheric Sciences over Africa (ICEMASA); and Mozambican Ministry of Science and Technology (grant PDRHCT) with assistance from the World Bank. The model simulations were ran using high performance computer (CORE) from join Climate System Analysis Group (CSAG) and Department of Oceanography at UCT. Altimetry data were distributed by AVISO, with support from CNES.

References

Backeberg, B.C., Reason, C.J.C., 2010. A connection between the South Equatorial Current north of Madagascar and Mozambique Channel eddies. Geophys. Res. Lett. 37 (4), L04604. http://dx.doi.org/10.1029/2009GL041950.

Barnier, B., Siefridt, L., Marchesiello, P., 1995. Thermal forcing for a global ocean circulation model using a three-year climatology of ECMWF analyses. J. Mar. Syst. 6 (4), 363–380. http://www.sciencedirect.com/science/article/pii/0924796394000349.

Biastoch, A., Krauss, W., 1999. The role of mesoscale eddies in the source regions of the Agulhas Current. J. Phys. Oceanogr. 29, 2303–2317.

Cai, S., Su, J., Gan, Z., Liu, Q., 2002. The numerical study of the South China Sea upper circulation characteristics and its dynamic mechanism, in winter. Cont. Shelf Res. 22 (15), 2247–2264. http://www.sciencedirect.com/science/article/pii/S0278434302000730.

Casey, K.S., Cornillon, P., 1999. A comparison of satellite and in situ − based sea surface temperature climatologies. J. Clim. 12 (6), 1848–1863. http://dx.doi.org/10.1175/1520-0442(1999)012<1848:ACOSAI>2.0.CO;2.

Chevane, C., Penven, P., Nehama, F., Reason, C., 2016. Modelling the tides and their impacts on the vertical stratication over the Sofala Bank, Mozambique. Afr. J. Mar. Sci. 38 (4), 465–479. http://dx.doi.org/10.2989/1814232X.2016.1236039.

Da Silva, A., Young-Molling, C., Levitus, S., 1994. Atlas of surface marine data 1994, vol. 1. In: Algorithms and Procedures, NOAA Atlas NESDIS, Vol. 6. Natl. Oceanic and Atmos. Admin., Silver Spring, Md.

Debreu, L., Marchesiello, P., Penven, P., Cambon, G., 2012. Two-way nesting in split-explicit ocean models: algorithms, implementation and validation. Ocean Model 49-50, 1–21.

Ducet, N., Le Traon, P.-Y., Reverdin, G., 2000. Global high-resolution mapping of ocean circulation from TOPEX/Poseidon and ERS-1 and -2. J. Geophys. Res. 105, 19477–19498.

Egbert, G., Erofeeva, S., 2002. Efficient inverse modeling on barotropic ocean tides. J. Atmos. Ocean. Technol. 19 (2), 183–204.

Falcieri, F.M., Benetazzo, A., Sclavo, M., Russo, A., Carniel, S., 2014. Po River plume pattern variability investigated from model data. Cont. Shelf Res. 87, 84–95. (oceanography at coastal scales). http://www.sciencedirect.com/science/article/pii/S0278434313003518.

Flather, R., 1976. A tidal model of the northwest European continental shelf. In: Memoires de la Society Royal des Sciences de Liegr 6 Series 10, pp. 141–161.

Gammelsrod, T., 1992. Variation in shrimp abundance on Sofala Bank, Mozambique, and its relation to the Zambezi River runoff. Estuar. Coast. Shelf Sci. 35, 91–103.

Garvine, R.W., 1987. Estuary plume and fronts in shelf waters: a layer model. J. Phys. Oceanogr. 17, 1877–1896.

Haidvogel, D.B., Beckmann, A., 1999. Numerical Ocean Circulation Modeling. Vol. 2 Imperial College Press.

Halo, I., Backeberg, B., Penven, P., Ansorge, I., Reason, C., Ullgren, J.E., 2014. Eddy properties in the Mozambique Channel: a comparison between observations and two numerical ocean circulation models. Deep-Sea Res. II Top. Stud. Oceanogr. 100 (0), 38–53. (the Mozambique Channel: Mesoscale Dynamics and Ecosystem Responses). http://www.sciencedirect.com/science/article/pii/S0967064513004098.

Hetland, R., 2004. Water mass structure of wind forced river plume. J. Phys. Oceanogr. 1–32.

Hickey, B., Geier, S., Kachel, N., MacFadyen, A., 2005. A bi-directional river plume: the Columbia in summer. Cont. Shelf Res. 25 (14), 1631–1656. http://www.sciencedirect.com/science/article/pii/S0278434305000786.

Horner-Devine, A., 2009. The bulge circulation in the Columbia River plume. Cont. Shelf Res. 29, 234–251.

Ivanov, B.G., Hassan, A.M., 1976. Penaeid shrimps (Decapoda, Penaeidae) collected off East Africa by the fishing vessel “Van Gogh”, 1. Solenocera ramadani sp. nov., and commercial species of the genera Penaeus and Metapenaeus. Crustaceana 30 (3), 241–251. http://www.jstor.org/stable/20103049.

Jakobsson, M., Macnab, R., Mayer, L., Anderson, R., Edwards, M., Hatzky, J., Schenke, H.W., Johnson, P., 2008. An improved bathymetric portrayal of the Arctic Ocean: implications for ocean modeling and geological, geophysical and oceanographic analyses. Geophys. Res. Lett. 35 (7), L07602. http://dx.doi.org/10.1029/2008GL033520.

Jin, B., Wang, G., Liu, Y., Zhang, R., 2010. Interaction between the East China Sea Kuroshio and Ryukyu current as revealed by self-organizing map. J. Geophys. Res. 115, 1–7.

Jose, Y.S., Aumont, O., Machu, E., Penven, P., Moloney, C.L., Maury, O., 2014. Influence of mesoscale eddies on biological production in the Mozambique Channel: Several contrasted examples from a coupled ocean-biogeochemistry model. Deep-Sea Res. II Top. Stud. Oceanogr. 100 (0), 79–93. (the Mozambique Channel: Mesoscale Dynamics and Ecosystem Responses). http://www.sciencedirect.com/science/article/pii/S0967064513004128.

Kohonen, T., 2001. Self-organizing Maps, 3rd Edition. Springer-Verlag, Berlin (number 30 in Springer Series in Information Sciences).

Large, W.G., McWilliams, J.C., Doney, S.C., 1994. Oceanic vertical mixing: a review and a model with a nonlocal boundary layer parameterization. Rev. Geophys. 32, 363–403.

Liu, Y., Weisberg, R.H., Mooers, C.N.K., 2006. Performance evaluation of the self-organizing map for feature extraction. J. Geophys. Res. 111, C05018.

Liu, Y., Weisberg, R.H., Yuan, Y., 2008. Patterns of upper layer circulation variability in the South China Sea from satellite altimetry using the self-organizing map. Acta Oceanol. Sin. 27, 129–144.

Lutjeharms, J.R.E., 2006. The Agulhas Current. Springer-Praxis Books.

Lutjeharms, J.R.E., Biastoch, A., van der Werf, P.M., Ridderinkhof, H., de Ruijter, W.P.M., 2012. On the discontinuous nature of the Mozambique Current. Afr. J. Mar. Sci. 108 (1/2), 1–5.

Malauene, B.S., Shillington, F.A., Roberts, M.J., Moloney, C.L., 2014. Cool, elevated chlorophyll-a waters off northern Mozambique. Deep-Sea Res. II Top. Stud. Oceanogr. 100 (0) (68-8). (the Mozambique Channel: Mesoscale Dynamics and Ecosystem Responses). http://www.sciencedirect.com/science/article/pii/S0967064513004116.

Marchesiello, P., McWilliams, J.C., Shchepetkin, A., 2003. Equilibrium structure and dynamics of the California current system. J. Phys. Oceanogr. 33, 753–783.

Mason, E., Molemaker, J., Shchepetkin, A.F., Colas, F., McWilliams, J.C., Sangra, P., 2010. Procedures for offline grid nesting in regional ocean models. Ocean Model 35 (1–2), 1–15. http://www.sciencedirect.com/science/article/pii/S146350031000082X.

Nehama, F.P.J., April 2012. Modelling the Zambezi River Plume Using the Regional Oceanic Modelling System (Ph.D. thesis). Department of oceanography - University of Cape Town, South Africa.

Nehama, F.P., Reason, C.J., 2014. Morphology of the Zambezi River plume in the Sofala

Bank, Mozambique. West. Indian Ocean J. Mar. Sci. 13 (1), 1–10.
Nehama, F., Reason, C., 2015. Modelling the Zambezi River plume. Afr. J. Mar. Sci. 37 (4), 593–604.
Penven, P., Chang, N., Shillington, F.A., 2006a. Modelling the Agulhas Current using SAfE (Southern Africa experiment). Geophys. Res. Abstr. 8 (Abstract 04225).
Penven, P., Debreu, L., Marchesiello, P., McWilliams, J.C., 2006b. Evaluation and application of the ROMS 1-way embedding procedure to the Central California upwelling system. Ocean Model 12, 157–187.
Penven, P., Marchesiello, P., Debreu, L., Lefevre, J., 2008. Software tools for pre- and post-processing of oceanic regional simulations. Environ. Model. Softw. 23 (5), 660–662. http://www.sciencedirect.com/science/article/pii/S1364815207001296.
Penven, P., Halo, I., Pous, S., Marie, L., 2014. Cyclogeostrophic balance in the Mozambique Channel. J. Geophys. Res. Oceans 119 (2), 1054–1067. http://dx.doi.org/10.1002/2013JC009528.
Quartly, G., de Cuevas, B., Coward, A., 2013. Mozambique Channel eddies in GCMS: a question of resolution and slippage. Ocean Model 63 (0), 56–67. http://www.sciencedirect.com/science/article/pii/S1463500312001886.
Ridderinkhof, H., de Ruijter, W.P.M., 2003. Moored current observations in the Mozambique Channel. Deep-Sea Res. II 50, 1933–1955.
Rio, M.H., Guinehut, S., Larnicol, G., 2011. New CNES-CLS09 global mean dynamic topography computed from the combination of GRACE data, altimetry, and in situ measurements. J. Geophys. Res. Oceans 116, C07018. http://dx.doi.org/10.1029/2010JC006505.
Risien, C.M., Chelton, D.B., 2008. A global climatology of surface wind and wind stress elds from eight years of QuikSCAT scatterometer data. jpo 38, 2379–2413.
Roberts, M.J., Ternon, J.-F., Morris, T., 2014. Interaction of dipole eddies with the western continental slope of the Mozambique Channel. Deep-Sea Res. II Top. Stud. Oceanogr. 100 (0), 54–67. (the Mozambique Channel: Mesoscale Dynamics and Ecosystem Responses). http://www.sciencedirect.com/science/article/pii/S0967064513004104.
de Ruijter, W.P.M., Ridderinkhof, H., Lutjeharms, J.R.E., Schouten, M.W., Veth, C., 2002. Observations of the flow in the Mozambique Channel. Geophys. Res. Lett. 29 (10), 1502–1504.
Sætre, R., da Silva, A.J., 1982. Water mass and circulation of the Mozambique Channel. In: Revista de Investigação Pesqueira. Tech. Rep. Vol. 3 Instituto de Desenvolvimanto Pesqueiro, Maputo.
Sætre, R., da Silva, A.J., 1984. The circulation of the Mozambique Channel. Deep-Sea Res. I 31, 485–508.
Schouten, M.W., de Ruijter, W.P.M., van Leeuwen, P.J., Ridderinkhof, H., 2003. Eddies and variability in the Mozambique Channel. Deep-Sea Res. II 50, 1987–2003.
Shchepetkin, A.F., McWilliams, J.C., 2005. The regional ocean modeling system (ROMS): a split-explicit, free-surface, topography-following-coordinate oceanic model. Ocean Model. 9, 347–404.
da Silva, J.C.B., New, A.L., Magalhaes, J.M., 2009. Internal solitary waves in the Mozambique Channel: Observations and interpretation. J. Geophys. Res. Oceans 114 (C5), 1–12. http://dx.doi.org/10.1029/2008JC005125.
de Sousa, L.P., Abdula, S., de Sousa, B.P., Penn, J., Howell, D., 2013. The Shallow Water Shrimp at Sofala Bank Mozambique 2013 (Unpublished report). Instituto Nacional de Investigação Pesqueira, Maputo.
Ternon, J.F., Roberts, M.J., Morris, T., Hancke, L., Backeberg, B., 2014. In situ measured current structures of the eddy field in the Mozambique Channel. Deep-Sea Res. II Top. Stud. Oceanogr. 100 (0), 10–26. (the Mozambique Channel: Mesoscale Dynamics and Ecosystem Responses). http://www.sciencedirect.com/science/article/pii/S0967064513004074.
Tew-Kai, E., Marsac, F., 2009. Patterns of variability of sea surface chlorophyll in Mozambique Channel: a quantitative approach. J. Mar. Syst. 77, 77–88.
Ullgren, J., Aken, H., Ridderinkhof, H., de Ruijter, W.P.M., 2012. The hydrography of the Mozambique Channel from six years of continuous temperature, salinity and velocity observation. Deep-Sea Res. I 69, 36–50.
Ullgren, J.E., Andre, E., Gammelsrod, T., Hoguane, A.M., 2016. Observations of strong ocean current events offshore Pemba, Northern Mozambique. J. Oper. Oceanogr. 9 (1), 55–66. http://dx.doi.org/10.1080/1755876X.2016.1204172.
Wehrens, R., Buydens, L.M.C., 2007. Self- and super-organizing maps in R: the Kohonen package. J. Stat. Softw. 21 (5), 1–19.
Weimerskirch, H., Le Corre, M., Jaquemet, S., Potier, M., Marsac, F., 2004. Foraging strategy of a top predator in tropical water: great frigatebirds in the Mozambique Channel. Mar. Ecol. Prog. Ser. 275, 297–308.
Zavala-Garay, J., Theiss, J., Moulton, M., Walsh, C., Woesik, R., Mayorga-Adame, C.G., García-Reyes, M., Mukaka, D., Whilden, K., Shaghude, Y., 2015. On the dynamics of the Zanzibar Channel. J. Geophys. Res. Oceans 120 (9), 6091–6113.
Zeng, X., Li, Y., He, R., Yin, Y., 2015. Clustering of loop current patterns based on the satellite-observed sea surface height and self-organizing map. Remote Sens. Lett. 6 (1), 11–19.